

Probing the dark ages with redshift distribution of GRBs

T. Roy Choudhury^{*}, R. Srianand[†]

IUCAA, Post Bag 4, Ganeshkhind, Pune 411 007, India.

3 November 2018

ABSTRACT

In this article, we explore the possibility of using the properties of gamma ray bursts (GRBs) to probe the physical conditions in the epochs prior to reionization. The redshift distribution of GRBs is modelled using the Press-Schechter formalism with an assumption that they follow the cosmic star formation history. We reproduce the observed star formation rate obtained from galaxies in the redshift range $0 < z < 5$, as well as the redshift distribution of the GRBs inferred from the luminosity-variability correlation of the burst light curve. We show that the fraction of GRBs at high redshifts, whose afterglows cannot be observed in R and I band due to HI Gunn Peterson optical depth can, at the most, account for *one third of the dark GRBs*. The observed redshift distribution of GRBs, with much less scatter than the one available today, can put stringent constraints on the epoch of reionization and the nature of gas cooling in the epochs prior to reionization.

Key words: cosmology: theory — early universe — gamma rays: bursts

1 INTRODUCTION

The usefulness of gamma ray bursts (GRBs) to probe the evolution of the universe is realized ever since the redshift measurements of GRBs became possible (Kulkarni et al. 1998). A direct connection between the GRBs and star formation rate (SFR) in the host galaxy is expected in the two popular models for GRB progenitors (collapsar and binary coalescence). There are also growing observational indications for the association of supernova-like components in several afterglows (Galama et al. 1999; Bloom et al. 1999). If indeed the rate of formation of GRBs is related to the SFR of host galaxy, they can be used as an effective probe of the star formation history of the universe (Lamb & Reichart 2000; Porciani & Madau 2001; Ciardi & Loeb 2000; Blain & Natarajan 2000; Bromm & Loeb 2002). Thus the redshift distribution of GRBs can complement the studies based on Lyman break galaxies in understanding the cosmic star formation history. At present only few tens of GRBs have redshift measurement and the list is, by no means, statistically complete. Recently it has been suggested that the redshift distribution of the GRBs can be probed using the global correlation that seems to exist between different observables of the afterglow. The redshift distribution of GRBs, albeit with large scatter, can be obtained using the correlation between GRB luminosity and variability (Fenimore & Ramirez-Ruiz 2000; Reichart et al. 2001; Lloyd-Ronning, Fryer, & Ramirez-Ruiz 2002).

The formation of galaxies and cosmic star formation histories have been studied extensively through analytical calculations and numerical simulations (see, for example, Rees & Ostriker (1977), White & Rees (1978), Katz, Weinberg, & Hernquist (1996), Gnedin

& Ostriker (1997), Chiu & Ostriker (2000)). These studies have been extended to investigate the cosmological implications of the GRBs. In this work, we take a simple model of the cosmic star formation history, based on Press-Schechter theory of collapsing haloes (in this work, the term ‘halo’ is used for referring to the dark matter halo) and elementary ideas on cooling and galaxy formation. The SFR density at low redshift in the model is constrained by the rest-UV luminosity observations of galaxies (Treyer et al. 1998; Cowie, Songaila, & Barger 1999; Steidel et al. 1999; Somerville, Primack, & Faber 2001). However, at high redshifts (say $z \geq 6$) the nature of reionization (viz. the epoch of reionization and nature of baryonic cooling in haloes) strongly influence the star formation history. The main aim of this article is to use observed redshift distribution of GRBs to probe the physical processes in the pre-reionization epoch. Indeed, one cannot probe this epoch directly in the optical wave band due to high Gunn-Peterson optical depth even if the intergalactic medium (IGM) is not completely neutral.

2 ANALYTICAL FORMALISM AND MODEL PARAMETERS

We use the Press-Schechter (PS) formalism to obtain the comoving number density of collapsed objects having mass in the range $(M, M + dM)$, which are formed at the redshift interval $(z_c, z_c + dz_c)$ and observed at redshift z (Sasaki 1994; Chiu & Ostriker 2000)

$$N(M, z, z_c) dM dz_c = N_M(z_c) \left(\frac{\delta_c}{D(z)\sigma(M)} \right)^2 \frac{\dot{D}(z_c)}{D(z_c)} \times \frac{D(z_c)}{D(z)} \frac{dz_c}{H(z_c)(1+z_c)} dM \quad (1)$$

^{*} E-mail: tirth@iucaa.ernet.in

[†] E-mail: anand@iucaa.ernet.in

where the overdot represents derivative with respect to time. The parameter $N_M(z_c)dM$ is the number of collapsed objects per unit comoving volume within a mass range $(M, M + dM)$ at redshift z_c , known as the PS mass function (Press & Schechter 1974), and δ_c is the critical overdensity for collapse, usually taken to be equal to 1.69 for a matter dominated flat universe ($\Omega_m = 1$). This parameter is quite insensitive to cosmology and hence the same value can be used for all cosmological models (Eke, Cole, & Frenk 1996). The other parameters are: $H(z)$ is the Hubble parameter, $D(z)$ is the growth factor for linear perturbations and $\sigma(M)$ is the rms mass fluctuation at a mass scale M .

At early epochs, (i.e., redshifts larger than the reionization redshift, $z > z_{re}$), the lower mass cutoff for the haloes which can host star formation will be decided by the cooling efficiency of the baryons. Indeed, the absence of heavier elements and lower free-zout molecular fraction of hydrogen ($f_{H_2} \simeq 10^{-6}$) in the primordial gas favours pure atomic cooling of the gas. This process can only make the gas cool upto 10^4 K. However, if one can somehow increase H_2 (and probably HD) content of the gas, the final temperature can be reduced which can lead to the formation of cold gas condensations within the low mass haloes (Tegmark et al. 1997). Density enhancement during the collapse of the haloes can increase the molecular fraction upto 10^{-4} in central parts of the haloes (Haiman, Abel, & Rees 2000). However, the Lyman and Werner band photons that are produced by luminous objects can easily destroy these H_2 molecules. Haiman, Abel, & Rees (2000) have shown that the haloes smaller than $T_{vir} = 10^{2.4}$ K cannot cool even in the absence of any Lyman and Werner band flux. In what follows we consider models with $T_{vir} = 300, 10^3$ and 10^4 K separately, which essentially covers the whole range of possibilities.

After the universe has been reionized ($z < z_{re}$), the lower mass cutoff for the haloes which are able to host star formation is set by the photoionization temperature ($T \simeq 10^4$ K). It is known from simulations that the photoionizing background suppresses galaxy formation within haloes with circular velocities less than 35 km s^{-1} , while the mass of cooled baryons is reduced by 50% for haloes with circular velocities $\sim 50 \text{ km s}^{-1}$ (Thoul & Weinberg 1996). However, the exact value will depend on the intensity and spectral shape of the ionizing background radiation. We consider this as a free parameter spanning a range of 35 km s^{-1} to 75 km s^{-1} for the circular velocity cutoff (v_c^{cut}). Note that v_c^{cut} is taken to be time-independent – hence, it does not correspond to the linear theory Jeans mass (which decreases with time) (Gnedin 2000). Also, in our model, the change from the neutral to reionized phase happens abruptly at $z = z_{re}$. However, in realistic models one needs to consider the transition region where considerable fraction of gas remains in the ionized phase. This will lead to an extra suppression in the low mass haloes even in the pre-overlapping era.

We assume that the SFR, of a halo of mass M which is formed at redshift z_c , is given by (Eggen, Lynden-Bell, & Sandage 1962; Cen & Ostriker 1992; Gnedin 1996)

$$\begin{aligned} \dot{M}_{SF}(M, z, z_c) &= \epsilon_{SF} \left(\frac{\Omega_b}{\Omega_m} M \right) \frac{t(z) - t(z_c)}{t_{dyn}^2} \\ &\times \exp \left[-\frac{t(z) - t(z_c)}{t_{dyn}} \right] \end{aligned} \quad (2)$$

where ϵ_{SF} is a efficiency parameter for the conversion of gas into stars. The function $t(z)$ gives the age of the universe at redshift z ; thus, $t(z) - t(z_c)$ is the age of the collapsed halo at z . We have assumed here that the duration of star formation activity in a given halo extends over a dynamical time-scale t_{dyn} . The exponential de-

crease of the SFR comes from the assumption that it is proportional to the mass of the cold gas (= total baryonic mass *minus* the mass already gone into stars) inside the halo (Schmidt's law). We use data obtained from rest-UV luminosities of galaxies, compiled and corrected for extinction by Somerville, Primack, & Faber (2001), to normalize ϵ_{SF} . Physically, this quantity depends on the metallicity of the gas and the effect of feedback due to outflows and local radiation field. For simplicity, we assume this to be independent of redshift for most of this article. Now we can write the cosmic SFR per unit comoving volume at a redshift z ,

$$\dot{\rho}_{SF}(z) = \int_z^\infty dz_c \int_M^\infty dM' \dot{M}_{SF}(M', z, z_c) \times N(M', z, z_c). \quad (3)$$

The lower mass cutoff M at a given epoch is decided by the Jeans criteria as explained above.

Assuming the formation GRBs is closely related to the formation of stars, we get the birthrate of GRBs at redshift z per unit comoving volume as

$$\phi(z) = f \dot{\rho}_{SF}(z) \quad (4)$$

where f is a efficiency factor which links the formation of stars to that of GRBs. It is the number of GRBs per unit mass of forming stars, hence it depends on the fraction of mass contained in (high mass) stars which are potential progenitors of the GRBs. This implies that f is crucially dependent on the slope of the stellar initial mass function (IMF).

Given the formation rate, it is straightforward to obtain the rate of GRB events per unit redshift range expected over the whole sky at present:

$$\frac{d\dot{N}^{GRB}}{dz} = \phi(z) \frac{1}{1+z} \frac{dV(z)}{dz} \quad (5)$$

where the factor $(1+z)$ is due to the time dilation between z and the present epoch, and $dV(z)$ is the comoving volume element

$$dV(z) = 4\pi c \frac{d_L^2(z)}{H(z)(1+z)^2} dz \quad (6)$$

The parameter $d_L(z)$ is the luminosity distance. Note that the difference between $\phi(z)$ and $d\dot{N}^{GRB}/dz$ is purely geometrical in nature. The number of GRBs per unit redshift range observed over a time Δt_{obs} is then given by

$$\frac{dN}{dz} = \frac{d\Omega}{4\pi} \Delta t_{obs} \Phi(z) \frac{d\dot{N}^{GRB}}{dz} \quad (7)$$

where $d\Omega/4\pi$ is the mean beaming factor and $\Phi(z)$ is the weight factor due to the limited sensitivity of the detector, because of which, only brightest bursts will be observed at higher redshifts.

3 RESULTS AND DISCUSSION:

The analysis presented here is based on LCDM model with the parameters $\Omega_m = 0.3, \Omega_\Lambda = 0.7, h = 0.65, \Omega_b h^2 = 0.02, \sigma_8 = 0.93, n = 1$. We consider three epochs of reionization (z_{re}), three virial temperatures (T_{vir}) upto which the gas can cool before reionization (i.e $z \geq z_{re}$) and three circular velocity cutoff (v_c^{cut}) for epoch after reionization. For a given set of model parameters, changing the reionization epoch is equivalent to changing the escape fraction of Lyman limit photons from the haloes. The SFR density obtained from our model is plotted as a function of redshift in Fig 1. In the panel (a) we plot the results for three epochs of reionization for $T_{vir} = 10^4$ K (solid curves) and 300 K (dashed curves) considering $v_c^{cut} = 35 \text{ km s}^{-1}$.

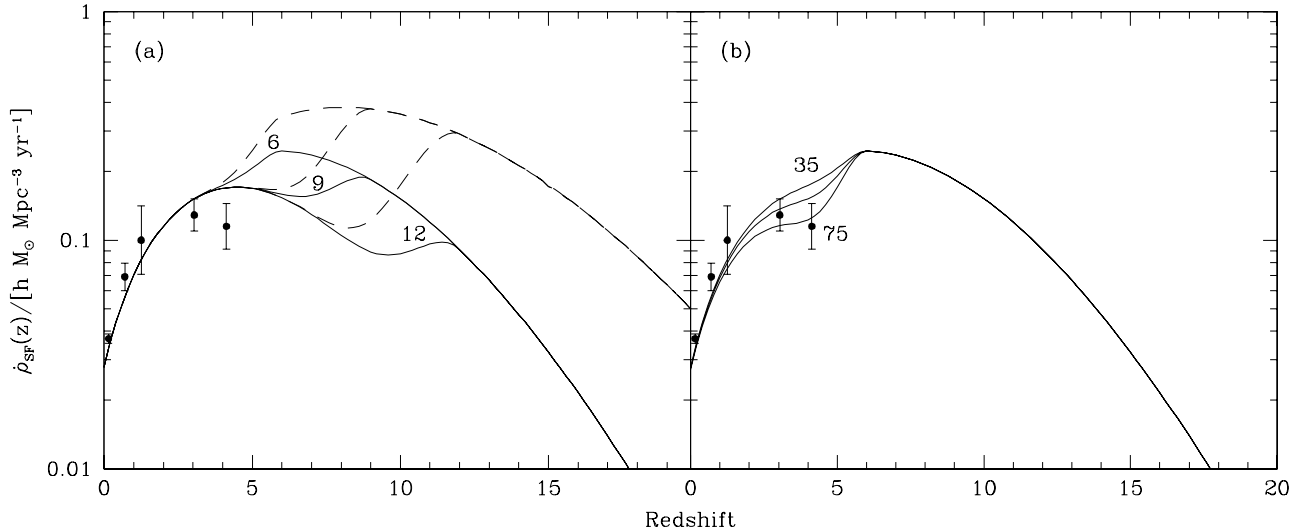


Figure 1. The SFR density as a function of redshift. In the panel (a) we plot the results for three epochs of reionization ($z_{\text{re}} = 6, 9$ and 12) for $T_{\text{vir}} = 10^4$ K (solid curves) and 300 K (dashed curves) considering $v_c^{\text{cut}} = 35 \text{ km s}^{-1}$. In panel (b) the results are plotted for $v_c^{\text{cut}} = 35, 50$ and 75 km s^{-1} considering $T_{\text{vir}} = 10^4$ K and $z_{\text{re}} = 6$. The curves are normalized using the extinction corrected data points from Somerville, Primack, & Faber (2001).

Our models consistently reproduce the observed points inferred from rest-UV luminosities of galaxies at $z \leq 5$ for ϵ_{SF} of 0.1 . Indeed the maxima in the curve occurs in the pre-reionization era. This is mainly due to the substantial contribution from the low mass haloes where the star formation is not suppressed by the photoionization (Barkana & Loeb 2000; Bromm & Loeb 2002). However, as expected, the SFR density depends strongly on the epoch of reionization and the nature of the cooling (hence T_{vir}). Interesting point to note is that across the reionization epoch there is upto 3 fold increase in the SFR density. This should be considered as a strict upper limit as is achieved when the Lyman and Werner band photons are completely absent (hence $T_{\text{vir}} = 300$ K). Additional difference of factor two could be introduced across z_{re} by increasing the v_c^{cut} to 75 km s^{-1} , thereby suppressing star formation in more low-mass haloes in the post-recombination era, which is shown in panel (b).

3.1 Dark GRBs:

The optical afterglows are only detected in one third of the well localized GRBs (Fynbo et al. 2001; Lazzati, Covino, & Ghisellini 2002; Reichart & Yost 2001). The GRBs without afterglows are called dark GRBs. The optical limits obtained in the case of dark afterglows are fainter than the detected ones. This suggests that the dark GRBs can not be accounted for by the failure to image deeply enough quickly (see Reichart & Price (2002) and references therein). The reason for these missing optical afterglows is attributed either (i) to the extinction in the host galaxy, or (ii) to the fact that some of the GRBs lie beyond the reionization epoch and the neutral IGM absorbs the afterglow. Indeed high- z QSO observations show complete Gunn-Peterson absorption for $z \geq 6$ QSOs (Fan et al. 2001; Djorgovski et al. 2001).

Our model predicts the redshift distribution of GRBs for a given f . Realistically, time evolution of the mass function of stars (for example triggered by the evolving metallicity) and the change in mean properties of the interstellar medium (ISM) will introduce time dependency for f . However, here we assume f to be constant.

To predict the *observed* redshift distribution, one needs to take into account the fact that only the brightest bursts will be observed at higher redshifts due to limited detector sensitivity. We take this into account by assuming a luminosity function of the form

$$\psi(L) \propto \left(\frac{L}{L_0}\right)^\gamma \exp\left(-\frac{L}{L_0}\right) \quad (8)$$

and then calculating the fraction of GRBs observed, $\Phi(z)$, at a particular z using the relation

$$\Phi(z) = \frac{\int_{L_{\text{min}}(z)}^{\infty} \psi(L) dL}{\int_0^{\infty} \psi(L) dL} \quad (9)$$

Here, L is the “isotropic equivalent” intrinsic burst luminosity in the energy band $30 - 2000 \text{ keV}$ (as defined by Porciani & Madau (2001)) and $L_{\text{min}}(z)$ is the corresponding minimum intrinsic luminosity that can be observed with the detector. We consider two separate cases – **Case A:** $\psi(L)$, and hence, L_0 is independent of z , and **Case B:** $\psi(L)$ evolves with redshift, with the evolution given by $L_0 \sim (1+z)^{1.4}$ as suggested by Lloyd-Ronning, Fryer, & Ramirez-Ruiz (2002).

For a given detector sensitivity, we can determine $L_{\text{min}}(z)$ from the relation

$$L_{\text{min}}(z) = P \frac{4\pi d_L^2(z) \int_{30 \text{ keV}}^{2000 \text{ keV}} ES(E) dE}{(1+z) \int_{(1+z)E_{\text{min}}}^{(1+z)E_{\text{max}}} S(E) dE} \quad (10)$$

where P is the minimum observed photon flux (sensitivity) at the detector in the energy band $[E_{\text{min}}, E_{\text{max}}]$ and $S(E)$ is the rest frame GRB energy spectrum. $S(E)$ is taken to be a broken power-law with a low-energy spectral index α , a high-energy spectral index β and a break energy E_b (Band et al. 1993). In this work, we take $\alpha = -1$ and $\beta = -2.25$, which are the mean values measured by Preece et al. (2000), and $E_b = 511 \text{ keV}$ (Porciani & Madau 2001).

The minimum intrinsic luminosity at z that can be observed by the detector depends on z in two ways: (i) the decrease in the flux due to distance and (ii) K-correction. For the luminosity function,

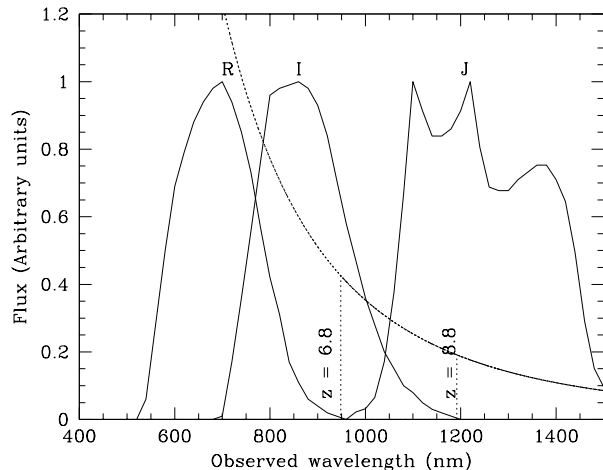


Figure 2. Powerlaw spectrum of GRB afterglow at different redshifts (labeled at emission wavelength of the Lyman- α line) modified by Gunn-Peterson effect of neutral IGM. The effect of damping wings is not considered here. We also plot the window function of the R, I and J bands. This figure illustrates the fact that afterglow will be invisible in R and I band for $z \geq 6.8$ and 8.8 respectively.

we take $\gamma = -2.5$, $L_0 = 3.2 \times 10^{51}$ ergs s^{-1} (which are obtained by Porciani & Madau (2001) using the $\log N - \log P$ relation for BATSE bursts) and $[E_{\min}, E_{\max}] = [50, 300]$ keV. We consider values of P corresponding to two detectors, namely, $P = 0.2$ photons $cm^{-2} s^{-1}$ (BATSE) and $P = 0.04$ photons $cm^{-2} s^{-1}$ (*Swift*) (Lamb & Reichart 2000).

A similar analysis needs to be carried out for the afterglows too. According to the simplest afterglow model of Wijers, Rees, & Meszaros (1997), the spectrum follows a power-law form when observed in the optical and X-ray wave-bands about 1 day after the burst. A simple analysis shows that the afterglow of the faintest detectable GRB will always be brighter than 23rd magnitude within 1 day after the burst in both I and R band. Hence, if a substantial fraction of GRB afterglows are not observed in I and R bands within 1 day after the burst, it must be because of radiative transfer effects and *not* because of cosmological effects.

We can now predict the percentage fraction of detectable GRBs at redshifts greater than z , called $F^{\text{GRB}}(z)$. From Fig 2, it is clear that due to high opacity of the IGM neither the afterglows nor the corresponding host galaxies will be detected in the R and I-band if the GRBs are located at $z \geq 6.8$ and 8.8 respectively. The fraction of R and I band dropout afterglows for a range of model parameters and detector sensitivities are given in the fourth to the seventh columns of the Table 1 ($F^{\text{GRB}}(\text{R})$ and $F^{\text{GRB}}(\text{I})$). The results clearly indicate that even in the optimistic case (with luminosity evolution and high sensitivity of the detectors), only 38% (25%) of the afterglows will not be detected in the R (I) band because of the extinction due to the IGM opacity. It is interesting to note that even if the HI optical depth of the ISM in the host galaxy is as high as $10^{23} cm^{-2}$, due to the redshift effect, X-ray absorption produced by this gas will not affect our visibility of this source in the soft X-ray band (0.5 to 2 keV) whenever it is detected in the hard X-rays. However such a gas will produce damped Lyman- α absorption.

Table 1. The predicted range in the percentage fraction of dark GRBs due to Gunn-Peterson effect, taking into account two different models for the luminosity evolution (Case A and B). The lower and upper limits of F are obtained with detector sensitivities similar to that of BATSE and *Swift* respectively.

z_{re}	v_c^{cut} km s^{-1}	T_{vir} K	$F^{\text{GRB}}(\text{R})$		$F^{\text{GRB}}(\text{I})$	
			Case A	Case B	Case A	Case B
6	75	10^4	0.8–3.9	15.5–25.6	0.2–0.9	5.6–11.4
6	50	10^4	0.8–3.5	14.1–23.7	0.2–0.8	5.1–10.5
6	35	10^4	0.7–3.3	13.3–22.5	0.1–0.7	4.8–10.0
6	35	10^3	1.1–5.0	20.0–32.9	0.3–1.4	8.8–17.7
6	35	300	1.3–5.7	22.7–36.9	0.4–1.7	10.7–21.1
9	35	10^4	0.6–2.7	12.3–21.8	0.1–0.7	5.2–11.1
9	35	10^3	0.9–4.1	19.1–33.3	0.3–1.5	10.1–20.7
9	35	300	1.0–4.7	22.1–37.9	0.4–1.8	12.4–24.9
12	35	10^4	0.4–1.9	8.7–16.1	0.0–0.5	3.7–8.4
12	35	10^3	0.5–2.3	12.3–24.0	0.2–0.9	7.3–16.7
12	35	300	0.5–2.5	14.3–28.0	0.2–1.1	9.2–20.9

3.2 Redshift distribution of GRBs:

We next compare the differential redshift distribution of GRBs with that obtained using the luminosity - variability ($L - V$) correlation of GRBs (Lloyd-Ronning, Fryer, & Ramirez-Ruiz 2002; Schaefer, Deng, & Band 2001). The variability V of a GRB gives a measure of the rms fluctuation of the burst light curve around the mean value. For the GRBs with known redshifts, it was seen that there is a correlation between the luminosity and the variability of the light curve, of the form $L \propto V^a$, with $a = 3.35^{+2.45}_{-1.15}$ (Fenimore & Ramirez-Ruiz 2000), $3.3^{+1.1}_{-0.9}$ (Reichart et al. 2001) and $1.57^{+0.48}_{-0.54}$ (Lloyd-Ronning, Fryer, & Ramirez-Ruiz 2002). The difference between various results is because of the precise definition of variability used. Since the number of GRBs with known redshifts is small (~ 20), the scatter in the ($L - V$) correlation is very large.

From this observed correlation, one can, in principle, obtain the redshift distribution of GRBs. Lloyd-Ronning, Fryer, & Ramirez-Ruiz (2002) use a sample of 220 bursts to obtain the intrinsic cumulative redshift distribution of GRBs $N_{\text{obs}}(< 1 + z)$. Their analysis, that corrects for the truncation effects in the sample due to limited detector sensitivities, gives the *intrinsic* redshift distribution of the GRBs. We distributed this data into logarithmic redshift bins and calculated the slope [which is essentially the differential distribution dN_{obs}/dz] for each bin. The error in each bin is mainly contributed by the scatter in the $L - V$ correlation.

The quantity predicted by our model dN/dz (given by eq (7), but without the factor $\Phi(z)$ in the right hand side) contains a normalization factor $f \Delta t_{\text{obs}} d\Omega / 4\pi$, which is fixed by fitting to the data using χ^2 -minimization technique. In Fig 3, we show the comparison between our predictions and the data obtained by Lloyd-Ronning, Fryer, & Ramirez-Ruiz (2002) using the $L - V$ correlation. Most of our models are broadly consistent with the data mainly because of large error bars. It is interesting to note that models with $T_{\text{vir}} \leq 10^3$ K deviate a lot from the mean observed points; but large errors, mainly from the large scatter in the $L - V$ relation, do not exclude these models. If the errors in the observed distribution reduce, one will be in a position to constrain the epoch of reionization and the contribution of molecular cooling (and other feedback mechanisms) in the formation of first generation of galaxies.

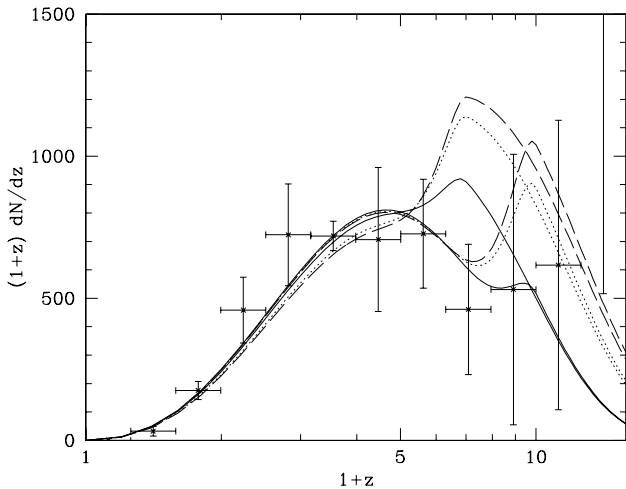


Figure 3. The redshift distribution of GRBs for different model parameters. The data points with error bars are from the observed $L - V$ correlation (Lloyd-Ronning, Fryer, and Ramirez-Ruiz 2002). The error bars along the y-axis represent the 1σ error due to the scatter in the observed $L - V$ correlation, while the error bars along the x-axis show the bin size. The results from our model are shown for $z_{re} = 6$ and 9, and for three different values of T_{vir} – namely, 10^4 K (solid curves), 10^3 K (dotted curves) and 300 K (dashed curves).

3.3 Discussions and Conclusions

In this article we have modelled the redshift distribution of GRBs assuming that they follow the cosmic star formation history. The main conclusions are summarized below:

- (i) A peak in the SFR before reionization is seen because of substantial contribution from the low mass haloes where the star formation is not suppressed by the photoionization (also noticed by Barkana & Loeb (2000) and Bromm & Loeb (2002)). We show that the redshift distribution of the SFR density depends on the reionization epoch and the minimum virial temperature (T_{vir}) of star forming haloes. The minimum virial temperature is set by the nature of the cooling – if H_2 cooling is effective, haloes with much lower virial temperatures can participate in the star formation.
- (ii) Our results clearly indicate that even in the optimistic case (with luminosity evolution and high sensitivity of the detectors), only 38% (25%) of the afterglows will not be detected in the R (I) band because of the extinction due to the IGM opacity. This means that a substantial fraction of optically dark GRBs ($\gtrsim 66\%$) originate because of effects such as dust extinction (Waxman & Draine 2000; Ramirez-Ruiz, Trentham, & Blain 2002; Berger et al. 2002).
- (iii) Although our predictions vary a lot as we change our model parameters, we cannot constrain the parameter space effectively because of large scatter in observations. One needs an improved observed redshift distribution to make real progress in understanding the physical processes in epochs prior to the reionization.
- (iv) In general, the efficiency parameters ϵ_{SF} and f depend of redshift. The star forming efficiency ϵ_{SF} evolves because of its dependence on the metallicity of the collapsing gas and the effect of feedback due to outflows and local radiation field. Similarly, the parameter f evolves as the stellar IMF becomes less top-heavy with decreasing z (Larson 1998). With improved observational data, one can use our model to constrain the evolution of these parameters.

One would naively expect that the presence of damping wing of HI absorption could be useful for probing the neutral IGM. How-

ever, in a simple picture of GRBs following supernovae, the presence of HII region and damped Lyman- α absorption because of the host galaxy will complicate the matter. Thus, we believe that the redshift distribution with less scatter may be a better way to probe the reionization.

We thank N. M. Lloyd-Ronning for providing us with data on the cumulative redshift distribution of GRBs. We also thank T. Padmanabhan for useful comments. T.R.C. is supported by the University Grants Commission, India.

REFERENCES

- Band D. et al., 1993, ApJ, 413, 281
 Barkana R., Loeb A., 2000, ApJ, 539, 20
 Berger E. et al., 2002, Preprint: astro-ph/0207320
 Blain A. W., Natarajan P., 2000, MNRAS, 312, L35
 Bloom J. S. et al., 1999, Nat, 401, 453
 Bromm V., Loeb A., 2002, Preprint: astro-ph/0201400
 Cen R., Ostriker J. P., 1992, ApJ, 399, L113
 Chiu W. A., Ostriker J. P., 2000, ApJ, 534, 507
 Ciardi B., Loeb A., 2000, ApJ, 540, 687
 Cowie L. L., Songaila A., Barger A. J., 1999, AJ, 118, 603
 Djorgovski S. G., Castro S., Stern D., Mahabal A. A., 2001, ApJ, 560, L5
 Eggen O. J., Lynden-Bell D., Sandage A. R., 1962, ApJ, 136, 748
 Eke V. R., Cole S., Frenk C. S., 1996, MNRAS, 282, 263
 Fan X. et al., 2001, AJ, 122, 2833
 Fenimore E. E., Ramirez-Ruiz E., 2000, Preprint: astro-ph/0004176
 Fynbo J. U. et al., 2001, A&A, 369, 373
 Galama T. J. et al., 1999, Nat, 398, 394
 Gnedin N. Y., 1996, ApJ, 456, 1
 Gnedin N. Y., 2000, ApJ, 542, 535
 Gnedin N. Y., Ostriker J. P., 1997, ApJ, 486, 581
 Haiman Z., Abel T., Rees M. J., 2000, ApJ, 534, 11
 Katz N., Weinberg D. H., Hernquist L., 1996, ApJS, 105, 19
 Kulkarni S. R. et al., 1998, Nat, 393, 35
 Lamb D. Q., Reichart D. E., 2000, ApJ, 536, 1
 Larson R. B., 1998, MNRAS, 301, 569
 Lazzati D., Covino S., Ghisellini G., 2002, MNRAS, 330, 583
 Lloyd-Ronning N. M., Fryer C. L., Ramirez-Ruiz E., 2002, ApJ, 574, 554
 Porciani C., Madau P., 2001, ApJ, 548, 522
 Preece R. D., Briggs M. S., Mallozzi R. S., Pendleton G. N., Paciesas W. S., Band D. L., 2000, ApJS, 126, 19
 Press W. H., Schechter P., 1974, ApJ, 187, 425
 Ramirez-Ruiz E., Trentham N., Blain A. W., 2002, MNRAS, 329, 465
 Rees M. J., Ostriker J. P., 1977, MNRAS, 179, 541
 Reichart D. E., Lamb D. Q., Fenimore E. E., Ramirez-Ruiz E., Cline T. L., Hurley K., 2001, ApJ, 552, 57
 Reichart D. E., Price P. A., 2002, ApJ, 565, 174
 Reichart D. E., Yost S. A., 2001, Preprint: astro-ph/0107545
 Sasaki S., 1994, PASJ, 46, 427
 Schaefer B. E., Deng M., Band D. L., 2001, ApJ, 563, L123
 Somerville R. S., Primack J. R., Faber S. M., 2001, MNRAS, 320, 504
 Steidel C. C., Adelberger K. L., Giavalisco M., Dickinson M., Pettini M., 1999, ApJ, 519, 1
 Tegmark M., Silk J., Rees M. J., Blanchard A., Abel T., Palla F., 1997, ApJ, 474, 1
 Thoul A. A., Weinberg D. H., 1996, ApJ, 465, 608
 Treyer M. A., Ellis R. S., Milliard B., Donas J., Bridges T. J., 1998, MNRAS, 300, 303
 Waxman E., Draine B. T., 2000, ApJ, 537, 796
 White S. D. M., Rees M. J., 1978, MNRAS, 183, 341
 Wijers R. A. M. J., Rees M. J., Meszaros P., 1997, MNRAS, 288, L51